DYNAMICAL COMPLEXITY ANALYSIS OF SACCADIC EYE MOVEMENTS IN TWO DIFFERENT PSYCHOLOGICAL CONDITIONS

C. AŞTEFĂNOAEI[1], D. CREANGĂ[1], E. PRETEGIANI[2], L. M. OPTICAN[3], A. RUFA[2]

[1] University "Alexandru Ioan Cuza", Faculty of Physics, Laboratory of Biophysics & Medical Physics, 11 Bd. Carol I, 700506, Iasi, Romania, corina_astefanoaei@yahoo.com
[2] University of Siena, Department of Medicine Surgery and Neuroscience, Eye-tracking &Visual Application Lab EVALab, Siena 53100, Italy
[3] National Eye Institute, Laboratory of Sensorimotor Research, Bethesda, MD, 20892, USA

Abstract. Saccadic eye movements of a normal subject were assessed through semi-quantitative analysis algorithms based on linear and non-linear test application in order to highlight the dynamics type characterizing saccadic neural system behavior. These movements were recorded during a simple visually-guided saccade test and one with a cognitive load involving button pressing to show a decision. Following the application of specific computational tests, chaotic dynamical trend dominancy was mostly revealed with some differences between the two saccade recording conditions: auto-correlation time was increased from 170 to 240 by cognitive task superposition and the Hurst exponent was enhanced from 0.52 to 0.76, denoting more persistence in the dynamics of saccadic system during increased neural activity related to cognitive task.

Key words: visually guided saccades, infrared eye tracking system, chaos theory, computational tests.

1. INTRODUCTION

Complex non-linear behavior in cellular membranes and physiological systems was shown two decades ago [1, 2], with special interest in chaotic neuron firing and related bifurcation behavioral issues [3, 4]. Chaos signature in neural cells and networks was found by mathematical approaching like the FitzHugh-Nagumo equations and the Hindmarsh-Rose equations [5, 6]. The extraction and processing of various temporal data series is very useful to distinguish between stochastic and chaotic processes. Computational tools based on Lyapunov formalism, attractor reconstruction and assessing its fractal dimension, surrogate data analysis etc. could be the alternative to traditional methods that failed to provide specific information on neural activity evolution. It seems that full

understanding of the various types of activities in neurons and neural sub-systems dynamics, the connections between them and the resulting behavioral patterns is not possible without computational interpretation of temporal series provided by different recording techniques. One of the most studied neural systems are those involved in visual information processing, since it represents about 80% of the information that human beings receive from the environment. Saccadic eye movements are necessary to quickly build an accurate representation of the visual field, as they bring the fovea – the part of the retina with the highest acuity – to objects of interest. Their study is important not only for physiology purposes but also for behavioral and pathological aspects. A statistical approach to eye saccades was reported by different researchers, like Collins *et al.*, 2009 [7], Federighi et al, 2009 [8], Rufa and Federighi, 2011 [9] that considerably contributed to description of physiological and pathological saccadic eye movement, especially in cerebellar ataxias.

In the analysis below we present a comparison between non-linear dynamics tests of two time series recorded for saccadic eye movements in two different psychological conditions: first, a simple saccadic task execution, and second, saccade execution with cognitive load, searching for the difference in dynamical dominant trend in each case. The application of mathematical algorithms designed for detecting non-linear behavior to eye movement signals may provide new information on related neuro-visual system, since a computational approach is an alternative way of understanding brain functioning; also, the presence of atypical response to computational tests of eye movement temporal series may be a useful indicator of specific pathology.

2. MATERIAL AND METHODS

2.1. EQUIPMENT AND EYE MOVEMENT RECORDING

The eye movement recordings were undertaken in one healthy adult subject that took part in experimental research developed in the Laboratory of Sensorimotor Research, National Eye Institute, National Institutes of Health, USA. The procedures followed NIH guidelines and were approved by the NIH institutional review board for human research. Subjects provided written, informed consent and were paid for their participation.

Saccadic eye movements were executed in response to two red spots visual stimuli (3 mm diameter) projected onto a translucent screen placed 105 cm in front of the subject's eyes. One spot was fixed, acting as central fixation point for the subject and the other one (target) could be moved at the left or at the right of the central fixation point. Horizontal and vertical eye movements were recorded from the right eye using an infrared iView X Hi-Speed camera (SMI) sampling at 1 kHz.

Only the horizontal movements were analyzed. Viewing was binocular. The subject's head was stabilized in the tracker by a chin rest and a forehead rest.

2.2. EXPERIMENTAL DESIGN

Subject took part in two recording sessions; each session took about 25-30 minutes. Every five-six minutes during the recording subject was given one-two minutes of rest time. In the first session, the subject was instructed to look at the central fixation point as soon as it came on and to maintain fixation until the appearance of the eccentric target. Then, he was asked to make a saccade to the target as quickly and accurately as possible. In the second session, the visual stimuli were the same as in the first session, but after looking at the target, the subject was requested to push one of two buttons, indicating whether he saw a gap by perceiving a period when no lights were on, or whether he saw an overlap by perceiving that both lights (central fixation point and the target) were on at the same time. This second session was meant to create an increased load at the cognitive level, which means an increased cerebral activity. For the computational study, a sequence of 10,000 data points was chosen.

2.3. THEORETICAL BACKGROUND

When analyzing biological signals, it is more probable that the type of dynamics will be masked by noise and artifacts, so it will not be clear to which general type of system the signal belongs [10]. Thus, it may not be prudent to rely on nonlinear features only, because the linear ones might provide additional information. Hence, a combined approach is usually preferred.

The strategy used here to investigate the neuro-visual system complexity is consistent with the application of the computational tests proposed by Sprott and Rowlands [11], which is a combination between linear and nonlinear tests, in order to assign the saccadic signal a behavioral type.

The power spectrum test involves a fast Fourier transformation of the recorded signal and measures the power (mean square amplitude) as a function of frequency.

The Fourier transform $F(\omega)$ of a time series $f(t)$ swaps the time variable with the frequency one giving a combination of slow and fast oscillations *i.e.* sinusoid functions, with different amplitude. High amplitude of low frequency component implies that there is a high correlation between the large-scale pieces of the signal in time (macro-structures); high amplitude of high frequency implies correlation in the micro-structures

$$F(\omega) = \int_{-\infty}^{\infty} X(t)e^{-j\omega t}dt \,, \tag{1}$$

with $j = \sqrt{-1}$. In contrast with infinite duration of theoretical signals we can define $F_T(\omega)$ which is the Fourier transform of the signal in time interval T, and define the power spectrum as following:

$$S_f(\omega) = \lim_{T \to \infty} \frac{1}{T}\left|F_T(\omega)\right|^2 \,. \tag{2}$$

The discrete Fourier transform of an array of N complex numbers $a_0, a_1, a_2, \ldots, a_{N-1}$ is a new N-periodic sequence of complex numbers $b_0, b_1, b_2, \ldots, b_{N-1}$ according to the formula:

$$b_n = \sum_{n=0}^{N-1} a_n \exp\left(-\frac{i2\pi kn}{N}\right), \tag{3}$$

with

$$a_n = \frac{1}{N}\sum_{n=0}^{N-1} b_n \exp\left(\frac{i2\pi kn}{N}\right) \tag{4}$$

representing the inverse Fourier transform. The power spectrum itself is the Fourier transform of the auto-correlation function:

$$\langle f(t)f(t+\tau)\rangle = \frac{1}{2\pi}\int_0^{\infty} S_f(\omega)e^{j\omega t}d\omega, \tag{5}$$

which represents the relationship of long and short-term correlation within the signal itself. The power spectrum being a function of frequency, it means that one can examine the long-term behavior of fast and slow oscillations.

Using a log-linear scale the visualization of the power spectrum of either random or chaotic data may be a broad spectrum but only chaotic signals are expected to emphasize a coherent decrease of the square amplitude with the frequency increase. The finger print of periodic and quasi-periodic systems is given by a few dominant peaks generated within the spectrum range.

The phase-space reconstruction is an important concept for the analysis of data generated by nonlinear dynamical processes. The phase-space is the space of all the possible equilibrium states toward which a physical system may evolve starting from different initial conditions but following the same laws. It is an abstract space with more than three dimensions, in which the state variables of the dynamic system form the axes [12]. As the dynamic system evolves in time, the state variables change their values, and trace out trajectories in this space. The

trajectory of a stable oscillating system will repeat itself, while that of a random system will haphazardly fill the space. Trajectories of a deterministic system cannot cross each other. A nonlinear deterministic system may have a strange attractor; the trajectories converge to a well-defined region of state space, but never repeat or cross themselves.

The autocorrelation function it's known as providing similar basic information as the power spectrum. It is a mathematical representation of the degree of similarity between a given time series and a lagged version of itself over successive time intervals. The autocorrelation time is given by the value of τ at which the autocorrelation function first falls to $1/e$. Increased values of autocorrelation time denote a high correlation in the signal, which is the hallmark of a chaotic dynamical component characterizing the data series. Autocorrelation can be exploited for predictions: an autocorrelated time series is predictable, probabilistically, because future values depend on current and past values.

The correlation dimension is a measure of the dimensionality of the space occupied by the attractor and gives an estimate of the attractor fractal dimension. It is obtained [13] by covering the series with boxes of a given size (r) and then computing the probability $p_i(r)$ of having a point of the series in the i-th such box. The correlation dimension is defined by:

$$CD = \lim_{r \to 0} \sum_i \frac{\log\left(\sum_i p_i r^2\right)}{\log r}. \tag{6}$$

The quantity $\sum_i p_i r^2$ is the probability of finding a pair of points in a box of size r, which is equal to the probability of having a pair of points with separation distance less than r, for small values of r. For large data series, of N points, the latter probability is given by the correlation sum:

$$C(r) = \lim_{N \to \infty} \frac{1}{N^2} \sum_{i,j=1}^{N} \theta\left(r - \left|X_i - X_j\right|\right), \tag{7}$$

where θ is the Heaviside step function: $\theta(x)=1$, for $x>0$, and $\theta(x)=0$, for $x<0$; $\left|X_i - X_j\right|$ is the separation distance between two points on the attractor, X_i and X_j. The multiplier $1/N^2$ is included to normalize the count by the number of pair of points on the attractor (without double counting). For small values of the separation distance (r), the correlation sum grows like a power such that:

$$C(r) \sim r^{CD}. \tag{8}$$

The "~" symbol is used here to indicate that this is a scaling relation, expected to be valid for sufficiently large N and small r. To find the value of CD, a

log-log plot of *C(r) versus r* is constructed, and the dimension is deduced from the slope of the curve over some range $r \leq r_0$. When the correlation dimension of the attractor stabilizes to a certain embedding dimension value, then the system is chaotic (if no stabilization occurs, then randomness is suspected to govern the system dynamics). Embedding dimension (*ED*) is the dimension of the state space, *i.e.* the number of states that are monitored at a particular moment in time. Procaccia [14] has shown that the number of points required to produce reliable correlation dimension predictions is $\sim 10^{CD}$, at least for high-quality data.

The Hurst exponent is a measure of the long-time correlations in a time series [15]. It is a dimensionless estimator for the self-similarity of the time series. To compute the Hurst exponent, these steps must be followed [16]: first, the rescaled range (*R/S*) is found for a range of values of the time series duration (*T*). The rescaled range is defined as the range of the data (*R*) – including the values from minimum to maximum – divided by the standard deviation (*S*); second, *R/S* is plotted as a function of *T* on a log-log plot. If the resulting graph is a straight line, the slope is the Hurst exponent:

$$H = \frac{\log(R/S)}{\log T} .$$ (9)

The values for Hurst exponent range between 0 and 1. For a purely random sequence (Brownian noise) with no correlation among intervals, $H = 0.5$. A value of $H \neq 0.5$ indicates autocorrelation in the signal: $H > 0.5$ means positive correlation or persistence, in the sense that large values are in general followed by large values, and small values by small values, on different time scales; values of $H < 0.5$ means negative correlation or anti-persistence such that large values are likely to be followed by small values, and vice versa, on the average over different time scales [17].

The Lyapunov exponents of a dynamical system are quantities that measure the rate of separation of infinitesimally close trajectories, a property of chaotic systems to be sensitive on initial conditions [18]. The maximal Lyapunov exponent is the most important since, if the difference between a pair of initial conditions has a nonzero component in the eigendirection associated with the largest eigenvalue, then that rate of divergence will dominate. It quantifies the average exponential divergence of nearby trajectories in state space where the sensitive dependence on initial conditions is obtained. Considering two points in a space, Z_0 and $Z_0 + \delta Z_0$, each generating a trajectory in that space using some equations or system of equations (Fig. 1). These trajectories can be considered as parametric functions of time. If one trajectory is used as reference, then the separation between the two trajectories will be also a function of time.
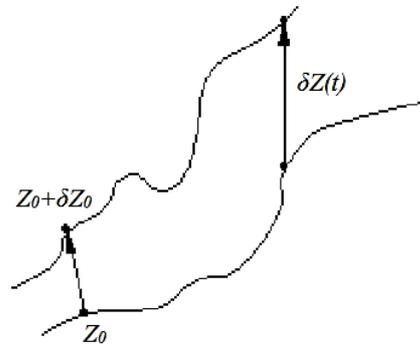
Fig. 1 – Separation of close trajectories [19].

The maximal Lyapunov exponent (LE) for a dynamical system can be defined as follows (eq. 10). The limit $\delta Z_0 \rightarrow 0$ ensure the validity of the linear approximation at any time [20].

$$\text{LE} = \lim_{\substack{t \rightarrow \infty \\ \delta Z_0 \rightarrow 0}} \frac{1}{t} \ln \frac{|\delta Z(t)|}{|\delta Z_0|} .$$ (10)

If LE < 0 then the orbit attracts to a stable fixed point or stable periodic trajectory – meaning (quasi) periodic dynamics; when LE = 0 the system is near a trajectory bifurcation being characterized not by stable but by an unstable state from which two evolution pathways are equally possible while for LE > 0, the trajectory is unstable and chaotic and the nearby points, no matter how close, will diverge to any arbitrary separation – meaning chaotic dynamics [11].

The above mentioned computational strategy was applied in the results section, to the raw data signals obtained from two types of recording sessions – normal, respectively cognitively loaded saccade execution – in parallel to the corresponding smoothed data series for each case.

3. RESULTS AND DISCUSSION

The angular shift data of the eye movement recorded during normal and cognitive load saccadic task execution are represented in Fig. 2, for raw signal. For simple execution of saccades, the graph shows some high amplitude fluctuations (marked by red circles on the graph), of about 20 degrees (Fig. 2, left), caused by involuntary eye blinking during the recordings. During cognitive load saccade recording (Fig. 2, right), the fact that the subject had to make a decision, by pressing a button, led to an increased neural activity which might be also related to the more accurate execution of the saccades – which is evident from the lack of blinks.
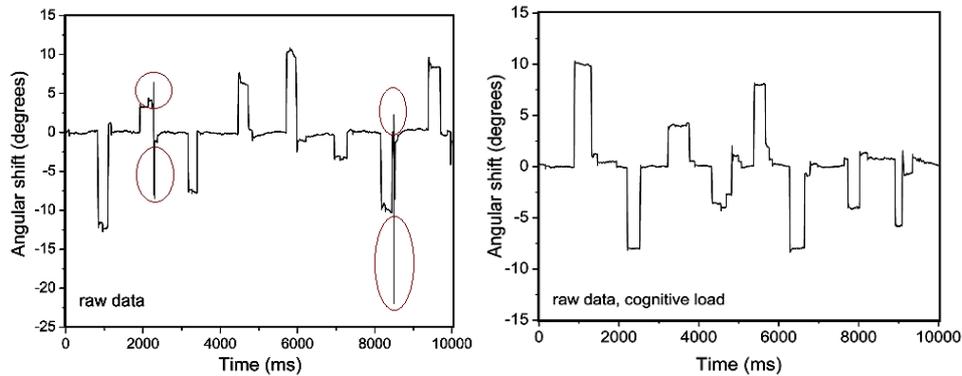
Fig. 2 – Angular shift of the eye during normal visually guided saccadic task (left)
and cognitive load one (right).

The probability distribution of the angular shift is given in Fig. 3, by means of box-plot representation. In the case of normal saccade data, it can be seen that by numerical smoothing, when every data point was replaced with the average value between that data and its two closest neighbors, the extreme outlier shifted to smaller absolute value while for cognitive load saccades no changes occurred.
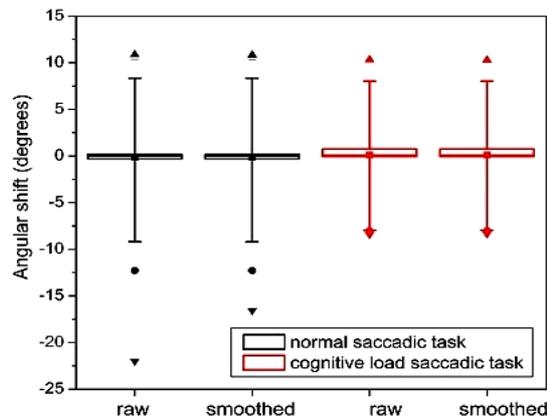
Fig. 3 – Box-plot representation of angular shift probability distribution, in normal and cognitive load saccadic task (circles for ordinary outliers and triangles for extreme outliers).

Compared to normal saccade recording in the case of cognitive load saccade execution the box length is slightly enlarged while the extreme outliers corresponding to negative angular shift have smaller absolute values being practically equal to the box corresponding tail edges – either for raw and smoothed data. This could be associated with the higher fluctuation amplitudes around the zero position – which would not be easy to see when inspecting the graphs from Fig. 2, and respectively with the blinking missing.

Representing the power spectrum of the studied signal in a linear-logarithmic scale, for both normal (Fig. 4, left) and cognitive load (Fig. 5, left) recordings, one could observed the decreasing of the power logarithm for low and medium frequency domain (up to 0.2), as it is indicated by the red lines on the graphs, which is the hallmark of a complex dynamical component characterizing the studied neuro-visual system.
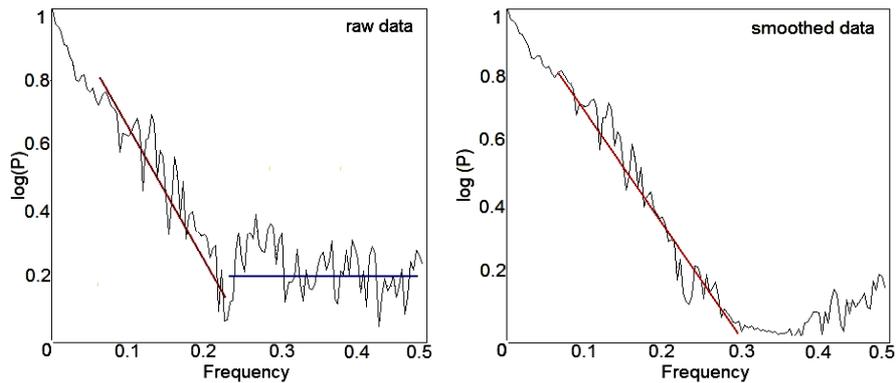
Fig. 4 – Linear-logarithmic plot of power spectrum for normal saccade execution;
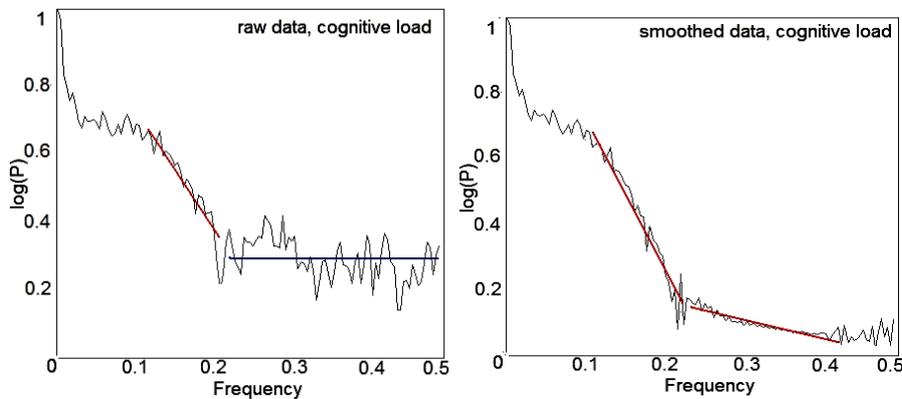P is the squared amplitude.

Fig. 5 – The power spectrum plot of cognitive load saccade execution,
in linear-logarithmic scale, for raw and smoothed data.

After numerical smoothing of the signal corresponding to normal saccades (Fig. 4 right), complex dynamics behavior could be observed also in larger frequency domain (up to 0.3). This chaos-like behavior is more evident in the case of normal saccadic task, as the slope is higher than in the case of cognitive load saccade execution.

In high frequency domain (between 0.2 and 0.5), the presence of a plateau (Fig. 4 left and Fig. 5 left) with some peaks in the spectrum (marked by the blue line on the graph) shows the dominancy of quasi-periodic behavioral trend. For cognitive load saccades (Fig. 5 right) a second linear decrease was noticed from 0.2 to 0.4 on the frequency scale – which possibly denotes different neural connections involved in relatively small frequency fluctuations and respectively high frequency ones; these could not be discriminated in the raw data because of recording noise.

The phase-space reconstructed using the temporal variation $X(t)$ of the studied system and its derivative, $X'(t)$, is shown in Figs. 6 and 7. In simple saccade execution session, the raw data presented large concentrically disposed polygonal lobes (Fig. 6, left) with asymmetrical appearance caused by certain high amplitude fluctuations (up to 10 degrees per second on X' axis) due to eye blinking.
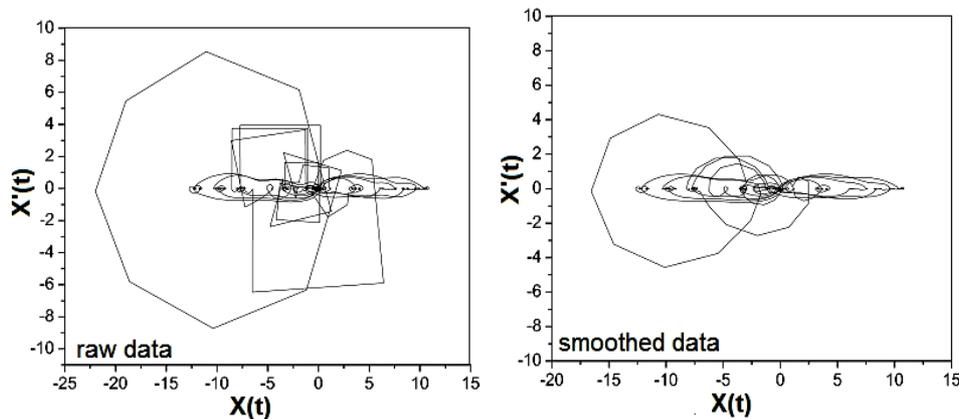

Fig. 6 – Phase-space portrait for normal condition saccade execution – the angular shift ($X(t)$) vs. its derivative ($X'(t)$).

Blinking fluctuation attenuation by signal smoothing resulted in the reducing of the attractor corresponding lobe size only up to the value of 5 degrees per second on X' axis (Fig. 6, right).

The increased cerebral activity caused by saccade execution with button pressing task related to target timing is supposed to give rise to a more controlled signal with a more regular attractor (Fig. 7). In this case, the lobes of the object shaped in the phase-space present evident bi-lateral symmetry, for both raw and smoothed data, which seems to suggest stronger deterministic or predictable patterns in the complex dynamics of the underlying neural saccadic system. Smoothing didn't change that symmetry.
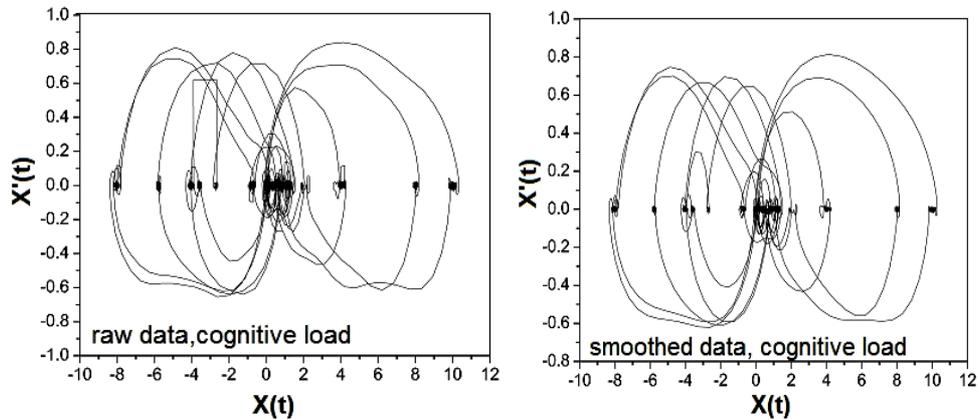
Fig. 7 – Phase-space portrait for cognitive load condition saccade execution – the angular shift (*X(t)*) *vs*. its derivative (*X'(t)*).

The main interpretation of these results concerns the complex chaotic dynamical feature of saccade series in both conditions; however from the different shapes of the phase-space portrait it could be assumed that different patterns of neural signal processing during saccade execution occur for simple visually guided saccades and the cognitive loaded ones.

The autocorrelation function for normal saccades and cognitive load saccade execution could be seen in Fig. 8 and Fig. 9. Significantly high values for the autocorrelation time, for both raw signals – τ_0 of about 170, and respectively 240 which indicates a considerable degree of correlation between the data in both recording conditions; smoothing didn't change that significantly – τ_0 of about 171, and respectively 240 were obtained.
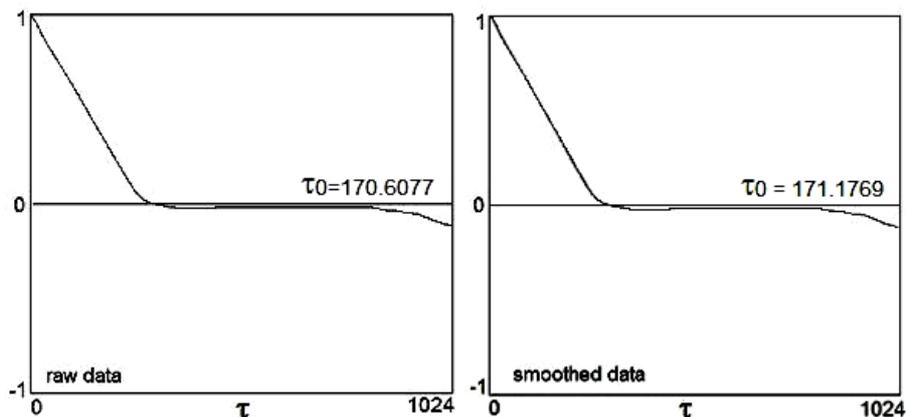

Fig. 8 – The autocorrelation function in simple saccadic task, for raw and smoothed data.

For comparison one may mention the case of Lorenz attractor [11] where the temporal series was theoretically generated as solution of an equation set describing pure chaotic dynamics with no evident periodic trend; there the autocorrelation time τ_0 was of about 5.8 *i.e.* thirty or forty times smaller than for the saccadic signals.

So one could say that saccadic eye movement signals are relatively highly correlated which is probably due to a linear dynamical component co-existing with the dominant chaotic dynamical trend. It is obvious that the cognitive load has increased the auto-correlation time with about 40% (Fig. 9), meaning that predictability of saccadic neuro-visual system was increased also.
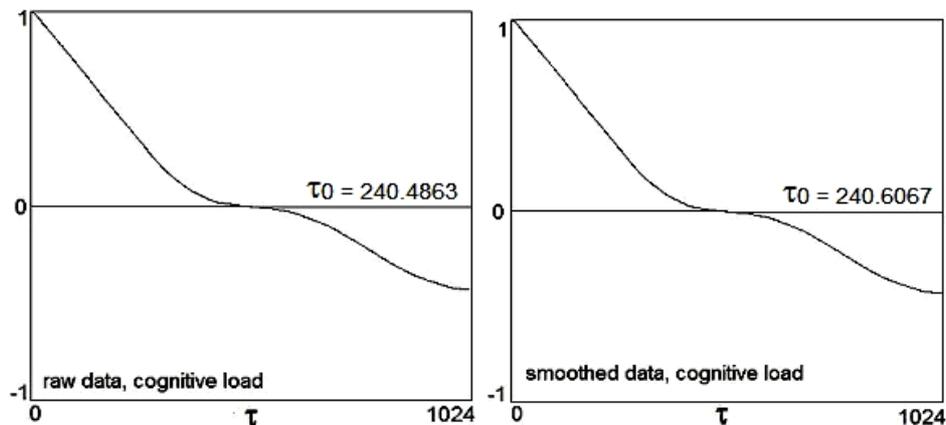

Fig. 9 – The autocorrelation function in cognitive load saccadic task, for raw and smoothed data.

The fractal dimension of the system attractor was assessed by the correlation dimension algorithm [11]. Plotting the correlation dimension (CD) as a function of the embedding dimension (ED) (Fig. 10), similar small values for the two recording sessions were obtained for both raw and smoothed data.

The graph shows a slight saturation tendency starting to a value over three for raw data while for smoothed data the estimated correlation dimension decreases to about 2.5 (Table 1). In the case of cognitive load raw data CD remains at about the same value (3.7) for ED from eight to ten (Table 1) while in the lack of cognitive task the stabilization of CD is evident only for ED equal to nine and ten – which suggests a possible better focalization of the subject on his saccadic test.

The CD value hasn't reach the value of four so that Proccacia condition is satisfied (since $N = 10^4$ points and CD $\sim$ lg$N$). One could observe that CD diminished by 1.5% to 3.8% in cognitive load condition for raw data (statistic non-significant, $p > 0.05$) and with 4.4% to 9.4% for corresponding smoothed data (statistic significant, $p < 0.001$) which can be related to certain simplification of saccadic task execution when cognitive load was imposed.

Table 1

Correlation dimension (CD) for consecutive embedding dimension (ED) for raw and smoothed data, in normal and cognitive load saccadic task

ED	Normal saccades Raw data	Normal saccades Smoothed data	Cognitive load Raw data	Cognitive load Smoothed data
1	-	1.104	-	1.049
2	2.154	1.740	2.107	1.635
3	2.655	1.971	2.616	1.785
4	2.602	2.149	2.447	2.054
5	2.920	2.244	2.876	2.119
6	3.273	2.550	3.197	2.431
7	3.406	2.704	3.310	2.559
8	3.441	2.611	3.755	2.626
9	3.818	2.871	3.714	2.694
10	3.781	3.115	3.635	2.950

The results seems to be in contrast with the report of Lamberts *et al.*, 2000 [21] that estimated increased correlation dimension in neural system during cognitive task performing – but they measured the global brain activity through electroencephalogram while we investigated specific neural system responsible for the execution of visually guided saccades.
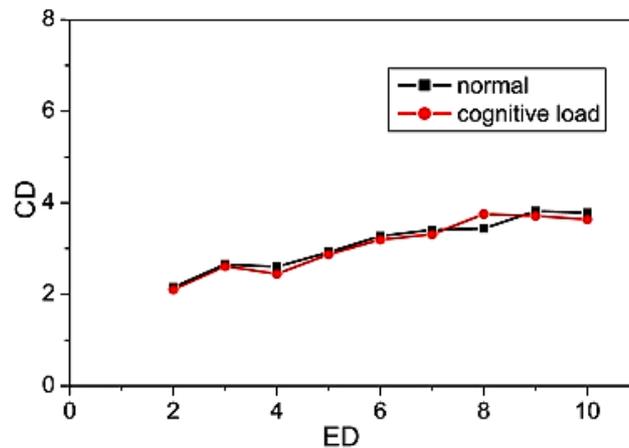

Fig. 10 – The correlation dimension (CD) *versus* embedding dimension (ED) for raw data in normal (black) and cognitive load (red) saccadic task.

The Hurst exponent test led to a value close to 0.5, obtained for raw data recordings for normal condition saccadic task (Fig. 11, left) that suggests rather a random walk in the data series, probably due to the fluctuations caused by involuntary eye blinks or by inherent noise of the recording system. After signal smoothing (Fig. 11, right), the Hurst exponent value shows higher correlation with a persistent behavior of the studied signal.
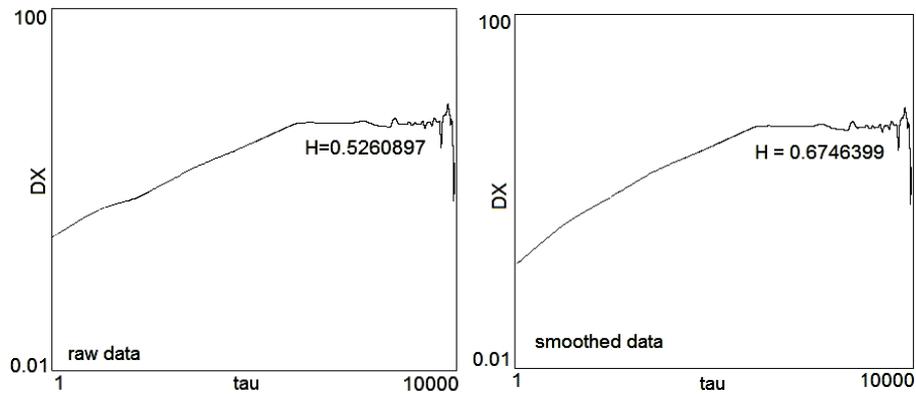
Fig. 11 – Hurst exponent for raw data and smoothed data in normal saccade execution.

Significant increase was noticed for cognitive load saccadic task, where probably the increased cerebral activity generated a higher degree of complexity in the saccadic response, denoted by the estimated values of Hurst exponent of 0.76 for raw data, respectively 0.77 for smoothed data (Fig.12). The interpretation could be related to the fact that the time series shows some memory, which makes sense, as one consider the experimental design with return to central fixation point after every saccade execution toward the target.
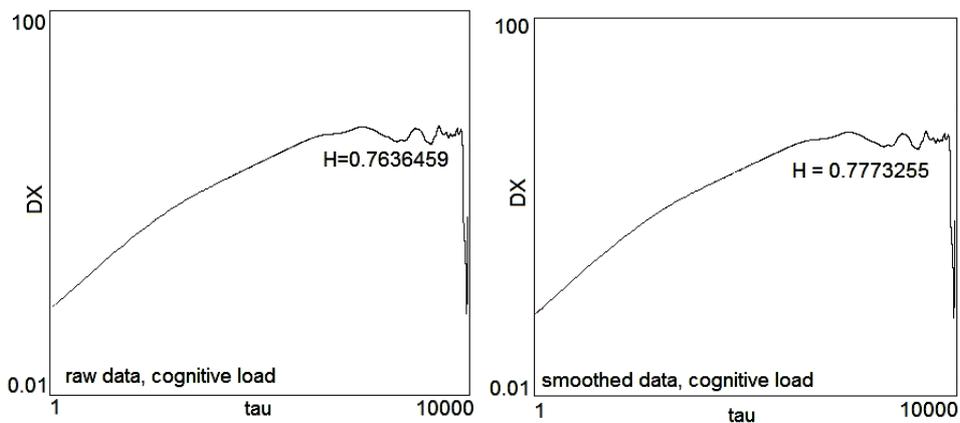

Fig. 12 – Hurst exponent for raw data and smoothed data in cognitive load saccade execution.

The maximal Lyapunov exponent computed for different ascending embedding dimensions [11], presented small (near-zero) positive values for both the simple saccadic test and the one with cognitive load. There were very small differences between the values obtained in these two recording conditions (Table 2), for raw data and also for the smoothed ones without statistic signification.

Table 2

Lyapunov exponent (*LE*) for consecutive embedding dimension (*ED*) for raw and smoothed data, in normal and cognitive load saccadic task

ED	Normal Raw data	Normal Smoothed data	Cognitive load Raw data	Cognitive load Smoothed data
1	1.239	0.955	0.372	0.344
2	0.276	0.066	0.078	0.035
3	0.095	0.034	0.046	0.029
4	0.066	0.033	0.035	0.029
5	0.042	0.028	0.028	0.031
6	0.035	0.027	0.025	0.030
7	0.028	0.028	0.023	0.027
8	0.023	0.027	0.025	0.027
9	0.026	0.028	0.026	0.029
10	0.025	0.027	0.024	0.029

Based on the near zero maximal Lyapunov exponent one may say that the neural system responsible for saccadic eye movements evolves close to a trajectory bifurcation. Its evolution leads to quasi-equilibrium states, from which two trajectories may evolve with equal probability – as a control parameter dictates. Each of these new trajectories can lead to new quasi-equilibrium states, and so on. This kind of evolution (Fig. 13) can be represented with the measured parameter, *X(t)*, on the ordinate and certain *r* parameter on the abscissa; such behavior resulting finally in chaotic dynamics for high *r* values.
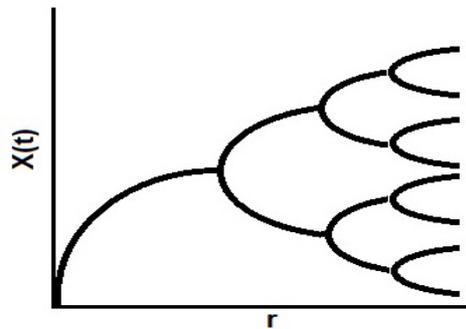

Fig. 13 – Bifurcated trajectories (after [22]).

From the view-point of quantity, the relation between *X(t)* and *r* is given solving a specific equations system, which describes the dynamics of the studied system. In our case, the steady states could be associated with neural cells resting potential – the states that cells return to after every saccade execution. Even if we actually measured muscle cells' activity (mechanical coupled with the electrical one) these effectors cells are controlled by afferent neural cells through neural

muscle junctions (NMJ) at the end of the neural circuitry responsible for saccade preparation, triggering and accomplishment.

We hypothesize that there is a simple (linear, deterministic) correlation between the cell membrane potential changes at the beginning of the neural circuitry (from the centers in frontal and parietal eye fields of the cerebral cortex, to the superior colliculus) and the ones at the end of this chain – which are involved in NMJ with muscle cells. A completely predictable functioning of the neural saccadic system would be based on a completely predictable behavior of any of its neurons; hence membrane electrical potential would reach exactly the same value every time a saccade is accomplished. On the contrary, less predictable transmission of neural information could be related to a control parameter r, monotonically varying along the neural circuitry and explaining bifurcation-like behavior.

Early experiments realized on giant squid axon showed that the resting potential depends on the fluctuations of ionic concentrations inside the axonal membrane. According to Goldman-Hodgkin-Katz equation, the resting potential depends on the Na^+ and K^+ cation concentration and also Cl^- anions concentration:

$$E_m = \frac{RT}{F} \ln \left(\frac{P_{Na^+}[Na^+]_{out} + P_{K^+}[K^+]_{out} + P_{Cl^-}[Cl^-]_{in}}{P_{Na^+}[Na^+]_{in} + P_{K^+}[K^+]_{in} + P_{Cl^-}[Cl^-]_{out}} \right), \tag{11}$$

where P_{ion} is the axonal membrane permeability for that ionic species, E_m is the membrane potential, $[ion]_{out}$ is the extracellular concentration of that ion, $[ion]_{in}$ is the intracellular concentration of that ion, R is the ideal gas constant, T is the temperature, and F is Faraday's constant. Bernstein's potassium hypothesis [23] states that potassium ions have a dominant role in generating the resting potential, so one may simplify the expression of E_m using Nernst equation and neglecting membrane permeability for Na^+ and Cl^-:

$$E_{K^+} = 61.5 \log ([K^+]_{out} / [K^+]_{in}). \tag{12}$$

The value of $RT/F = 61.5$ mV was calculated for normal body temperature (37ºC). One could assume that stochastic fluctuations of $[K^+]_{out}$ and/or $[K^+]_{in}$ concentrations, may lead to complex, chaotic variations of E_{K^+} which is found in less predictable (oscillatory) resting potential behavior. Yet, although the membrane permeability for potassium, P_{K^+}, is not explicitly present in Nernst equation, the variation of K^+ ions concentration could take place only through the variation of membrane permeability – and, actually, it is known that membrane ionic channels activation has a pronounced stochastic behavior [24].

Hence the presumption one could make based on near zero Lyapunov maximal exponent is that the resting potential doesn't remain at a stable value but it can oscillate between different values – which is valid for all the neurons in the neural circuitry involved in saccadic response.

The investigations (biophysical and computational) we performed until now don't provide information about the nature or variation of parameter r, which could control the supposed unpredictable behavior of $X(t)$ – angular shift of the eye. Further computational studies are needed to reveal putative differences in bifurcation like behavior for normal saccades and cognitive load ones.

4. CONCLUSION

The analysis of visually guided saccadic eye movements through computational methods was meant to reveal differences between normal saccades and cognitively loaded ones. First, involuntary blinking was less present in cognitive load saccadic tasks. Then, auto-correlation function, power spectrum and portrait in the phase-space appeared different in the two conditions denoting more predictability for cognitive load saccades. Correlation dimension and maximal Lyapunov exponent did not lead to significant differences. Dominant chaotic trend was shown to underline the dynamics of neural system responsible for saccadic eye movements as those presented in the experiment above new investigations being needed to study the influence of increased neural activity on the saccade execution.

REFERENCES

1. T. Elbert, W.J. Ray, Z.J. Kowalik, J.E. Skinner, K.E. Graf, N. Birbaumer, Physiol. Rev., **74**, 1–47 (1994).
2. H. Korn, P. Faure, C. R. Biol., **326**, *9*, 787–840 (2003).
3. T.R. Chay, Y.S. Fan, Y.S. Lee, International Journal of Bifurcation and Chaos, **5**, *3*, 595–635 (1995).
4. N.F. Rulkov, Phys. Rev. Lett., **86**, 183–186 (2001).
5. R. FitzHugh, *Mathematical models of excitation and propagation in nerve* (Chapter 1), in H.P. Schwan, ed. *Biological Engineering,* McGraw–Hill Book Co., NY, 1969, pp.1–85.
6. E.M. Izhikevich, Dynamical systems in neuroscience, *The MIT Press*, Cambridge, 2007.
7. T. Collins, A. Semroud, E. Orriols, K. Doré-Mazars, Invest Ophthalmol Vis Sci., **49**, *2*, 604–12 (2008).
8. P. Federighi, G. Cevenini, M.T. Dotti, E Pretegiani, A. Federico, A. Rufa, Brain, **134** (Pt 3), 879–9 (2011).
9. A. Rufa, P. Federighi, Annals of NY Academy of Sciences, **1233**, 148–154 (2011).
10. A. Jovic, N. Bogunovic, 15th IEEE Mediterranean Electrotechnical Conference, 2010, pp. 1340–1345.
11. J.C. Sprott, G. Rowlands, *Chaos Data Analyzer*, American Institute of Physics, New York, 1994.
12. M. Shelhamer, Journal of Neuroscience Methods, **83**, 45–56 (1998).
13. P. Grassberger, I. Procaccia, Physical Rewiew Letters, **50**, *5* (1983).
14. I. Procaccia, Nature, **333**, 498–9 (1988).

15. H.E. Hurst, Trans. Am. Soc. Civ. Eng., **166**, 770 (1951).
16. M. Shelhamer, W.M. Joiner, J. Neurophysiol, **90**, 2763–2769 (2003).
17. L. Telesca, V. Cuomo, V. Lapenna, M. Macchiato, Tectonophysics, **330**, 93–102 (2000).
18. J. Theiler, J. Opt. Soc. Am. A, **7**, *6* (1990).
19. *** http://hypertextbook.com/chaos/43.shtml
20. M. Cencini, F. Cecconi, A. Vulpiani, World Scientific, Singapore, 2010.
21. J. Lamberts, P.L.C. van den Broek, L. Bener, J. van Egmond, R. Dirksen, A.M.L. Coenen, Neuropsychobiology, **41**, 149–153 (2000).
22. *** http://www.schuelers.com/ChaosPsyche/part_1_7.htm
23. Kenneth Stewart Cole, *Biographical Memoirs of Fellows of the Royal Society*, **38**, *99–110*, 104 (1992).
24. B. Hille, *Channels of Excitable Membranes*, 2nd Ed., Sinauer, Sunderland, MA, 2001.